M. A. Latcha
University Graduate Fellow.

A. Akay
Professor.

Department of Mechanical Engineering,
Wayne State University,
Detroit, MI 48202

Application of the Helmholtz Integral in Acoustics

The solution of an isoparametric, overdetermined formulation of the Helmholtz Integral is presented and demonstrated in three examples of acoustic radiation from spherical sources. The placement of the interior, overdetermining points is discussed and guidelines concerning surface element size are developed and tested. The total radiated sound power and transient acoustic response of a dilating sphere are computed.

Introduction

In the design of mechanical systems, it is desirable to predict sound radiation characteristics of the system at the preliminary design stage. Although methods to predict the vibration response are often available, sound prediction techniques are not yet fully developed and implemented, in part due to the unresolved difficulties associated with the existing methods. Depending on the configuration of the surface of the source and the complexity of the surface vibration, a closed-form solution is often not possible. The Helmhotz integral is used as a basis for numerical techniques to solve problems of radiation from arbitrary surfaces. This integral, however, possesses mathematical and numerical difficulties that must be taken into consideration in the solution of radiation problems. The purpose of this paper is to highlight some of these difficulties and demonstrate how they might be alleviated.

Early work in the field of acoustic radiation from arbitrary bodies involved the use of approximate methods to find a distribution of simple acoustic sources to replace the surface of the body. Oestreicher [1] used the Helmholtz integral together with a Taylor expansion of the free-space Green's function to find analytical expressions for the source distributions. Horton and Innis [2] employed measurements of pressure and approximations of the velocity near the surface of a body in order to predict the far-field acoustic radiation.

As digital computers began to have more widespread use in research and industrial applications, investigators began to evaluate the Helmholtz integral directly. Chen and Schweikert [3] obtained acoustic pressure radiation patterns by solving part of the Helmholtz integral for only the "monopole" source distribution on the surface of the body being studied. Chertock [4] used the complete Helmholtz integral to numerically solve for the surface pressure distribution of problems with spherical symmetry. Copley [5] solved problems with axisymmetric geometry also using the complete Helmholtz Integral.

The Helmholtz integral does not possess a unique solution at certain frequencies corresponding to the eigenfrequencies of a related problem of the interior volume of the body in question. This is shown in references [6-10]. Two techniques have been developed to circumvent this difficulty. Schenck [8] combined the Helmholtz integral with the related Interior Helmholtz integral to identify solutions at these degenerate frequencies. Ursell [9] removed this nonuniqueness problem by reformulating the Green's function for each problem. Using the properties of the Helmholtz equation, Brod [10] changed the form of the Helmholtz integral to a relation that is unique for all wavenumbers.

Bell, Meyer, and Zinn [11] used both two- and three-dimensional forms of the Helmholtz Integral with various boundary conditions and geometric shapes to determine acoustic potentials at both the geometric boundaries and field points. The related surface Helmholtz integral was solved by Koopman and Benner [12, 13] as a step toward calculating the total radiated sound power. They used the concepts devised by Schenck [8] to eliminate the nonuniqueness problem.

One characteristic of the studies given in references [2-5, 8, 11-13] is that in the discretization of the boundary surfaces it was assumed that the acoustic variables were constant over each elemental area of the body surface. However, Seybert, et al. [14, 15] employed an isoparametric formulation of the Helmholtz integral to achieve solutions with accuracies comparable to those obtained in the foregoing studies with fewer surface elements, and therefore with less computation time.

The present work discusses, through examples, difficulties that arose in the earlier studies and the techniques and guidelines developed to alleviate some of these problems. It is also shown that once the Helmholtz integral is solved for the surface pressure response, it is a fairly simple task to obtain other quantities describing the acoustic field. This is done through two applications: The calculation of the total radiated sound power and the temporal acoustic response.

The Helmholtz Integral

In most of the aforementioned studies a brief derivation of the Helmholtz integral can be found. For a more detailed and complete development, reference [16] is excellent. The Helmholtz integral, as applied to the problems of acoustic radiation, is given here as

$$C(P)p(P) = \int_S [p\partial(e^{-ikr}/r)/\partial\nu + ikz_0 v_\nu e^{-ikr}/r]d\sigma \qquad (1)$$

where $i=\sqrt{-1}$, p and v are the complex-valued functions of acoustic pressure and velocity, S is the surface of the vibrating body with outward normal ν, $d\sigma$ is a differential element of surface area, k is the wavenumber, z_0 is the specific acoustic impedance of the surrounding infinite medium and r is the distance from the arbitrary point P to the integration point on the surface S. The subscript on the velocity denotes the

Contributed by the Noise Control and Acoustics Division for publication in the JOURNAL OF VIBRATION, ACOUSTICS, STRESS, AND RELIABILITY IN DESIGN. Manuscript received at ASME Headquarters, June 20, 1986.

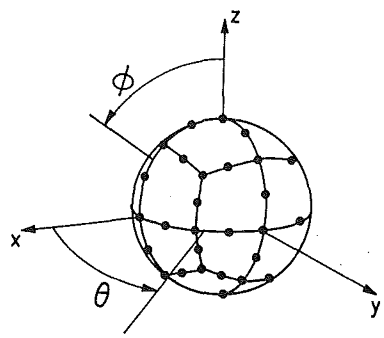

Fig. 1 Spherical model

derivative along the outward normal to the surface and the function $C(P)$ takes the values of 4π when P is outside of surface S, 2π when P is at a point of S where a unique normal tangent plane exists, and zero when P is inside of surface S. A generalization of this formulation can be found in references [14, 15]. Through a similar derivation utilizing Laplace's equation and a geometrical argument, the function $C(P)$ can be interpreted as the outer solid angle to surface S at point P. Equation (1) then takes the general form

$$\{4\pi+\int_S[\partial(1/r)/\partial\nu]d\sigma\}p(P)$$
$$=\int_S[p\partial(e^{-ikr}/r)/\partial\nu+ikz_0v_\nu e^{-ikr}/r]d\sigma \qquad (2)$$

The major obstacle in the solution of equation (2) is the evaluation of the surface integrals. This difficulty can be overcome analytically for certain special spherical geometries. More general geometries can be handled numerically by approximating the surface geometry using interpolation functions [14, 15].

Description of the geometry using interpolation, or shape, functions involves one basic idea: The geometric properties at a point can be expressed as a weighted sum of the corresponding properties at a given set of nearby points, called nodes. This weighted sum is of the form

$$x=\sum_{n=1}^{N}x_nh_n(r,s) \qquad (3)$$

where (r, s) are the natural coordinates of a local coordinate system, x_n is the property value of the nth node based on the global coordinate system, and h_n is the corresponding interpolating function of the local coordinates (r, s).

The use of interpolation functions is not limited to the description of geometric shapes, but can be extended to describe any variable present in the problem formulation. Variables such as velocity, acoustic pressure, stress, strain, etc., can be described using nodal values and corresponding sets of interpolating functions. If the same set of interpolation functions, and hence the same set of nodal coordinates, is chosen for every variable in each element, the problem becomes an isoparametric formulation.

To apply the concept of isoparametric formulation to equation (2), the first step is to discretize the surface S into M elements. It should be noted that this step does not introduce any approximations.

$$\left\{4\pi+\sum_{m=1}^{M}\int_{S_m}[\partial(1/r)/\partial\nu]d\sigma\right\}p(P)$$
$$=\sum_{m=1}^{M}\int_{S_m}[p\partial(e^{-ikr}/r)/\partial\nu+ikz_0v_\nu(e^{-ikr}/r)]d\sigma \qquad (4)$$

The second step is to substitute the approximations

$$p=\sum_{n=1}^{N}p_nh_n,\quad v_\nu=\sum_{n=1}^{N}v_{\nu n}h_n$$

into equation (4), which results in

$$\left\{4\pi+\sum_{m=1}^{M}\int_{S_m}[\partial(1/r)/\partial\nu]d\sigma\right\}p(P)$$
$$-\sum_{m=1}^{M}\sum_{n=1}^{N}p_n\int_{S_m}h_n[\partial(e^{-ikr}/r)/\partial\nu]J_nd\sigma$$
$$=ikz_0\sum_{m=1}^{M}\sum_{n=1}^{N}v_{\nu n}\int_{S_m}h_n(e^{-ikr}/r)J_nd\sigma \qquad (5)$$

where J_n is the Jacobian of the local-global coordinate transformation.

All of the surface integrals in equation (5), even though they involve surface normals that do not uniquely exist at edges and corners, can be successfully carried out if the surface is discretized in a manner such that all of the edges and corners of the model are on the boundaries of the elements.

Equation (5) is a form of equation (2) that allows the convenient computation of the acoustic radiation from any vibrating body with general geometry and arbitrary surface velocity distribution.

Solution of the Helmholtz Integral

Several numerical considerations must be kept in mind while solving the general Helmholtz integral, given by equation (5). Some of these are direct consequences of the form of the Helmholtz integral while others result from the numerical techniques commonly employed. This section discusses the problems encountered in earlier studies and describes how they are resolved in the present work.

Inspection of equation (5) shows that the acoustic pressure at a point P outside of surface S cannot be obtained without first the knowledge of both the normal velocity and the surface acoustic pressure distributions. These two distributions are not independent and are easily related through the Surface Helmholtz integral, which is obtained when point P in equation (5) is on the surface, S. When the normal velocity distribution is given (always the case in this paper), the first step in obtaining the acoustic pressure at an arbitrary field point consists of solving for the acoustic pressure distribution on the surface of the body.

The solution of the Surface Helmholtz integral in earlier studies was hindered by two main difficulties. The first problem was due to the singularities that occur at $r=0$ in both of the surface integrals of equation (5), in particular where numerical integration schemes were employed which required evaluation of the integrands at the singular points. The most convenient way to avoid this difficulty is to use a numerical integration scheme that does not require the evaluation of the integrands of equation (5) at the singular points. One such method is Gaussian quadrature [17]. Gaussian quadrature is also useful since it allows straightforward implementation of higher-order integration schemes for verification of the convergence of the singular integrals. The integration method employed in the examples presented in later sections is standard Gaussian quadrature for quadralateral regions, while the scheme used for integration over triangular regions is a variation of Gaussian quadrature developed by Cowper [18].

The second difficulty encountered in the solution of the Surface Helmholtz integral was that equation (5) fails to yield a unique solution for the surface acoustic pressure distribution at the eigenfrequencies of a related interior problem. This nonuniqueness problem is due only to the mathematical form of the Surface Helmholtz integral and seems not to have any physical significance. Schenck [8] has an excellent discussion of these characteristics and their effect on the solution of the Surface Helmholtz integral. Reference [8] also presents an improved formulation for the solution of the surface pressure distribution consisting of the combination of the Surface Helmholtz integral with the Interior Helmholtz integral. This combination results in an overdetermined set of simultaneous

Table 1 Results of surface area calculations for six different spherical models

Model Description	Calculated Surface Area % Difference from Theory
8 quadratic triangles, 18 nodes	-20.64%
32 quadratic triangles, 66 nodes	-14.19%
48 quadratic triangles, 98 nodes	-13.74%
72 quadratic triangles, 146 nodes	-13.54%
8 quadratic quadralaterals, 26 nodes	-5.80%
24 quadratic quadralaterals, 74 nodes	-0.95%

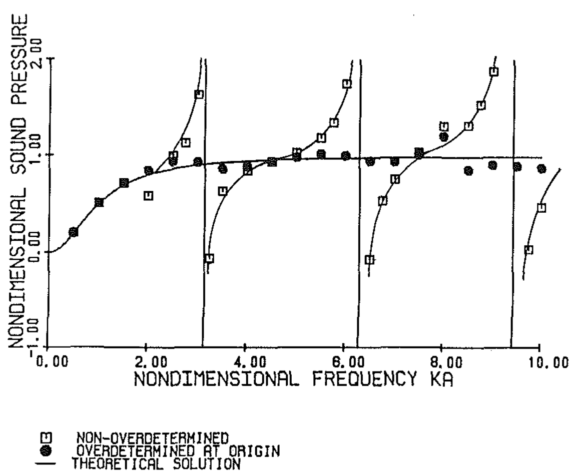

Fig. 2 Nondimensional surface pressure versus *ka* for the case of the dilating sphere

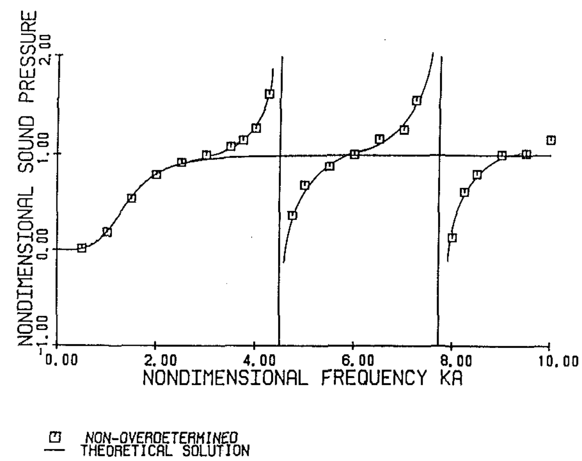

Fig. 3 Nondimensional surface pressure versus *ka* for the case of the oscillating sphere; $\phi = 0$

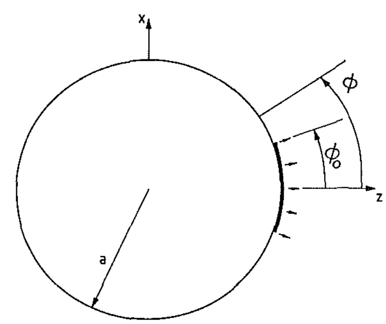

Fig. 4 Geometry for equation (12)

equations that, depending on the choice of interior points, insures a unique solution for the surface acoustic pressure distribution.

In the Surface Helmholtz integral, since point P is on the surface S, equation (5) is a Fredholm equation of the second kind [8] and is in a form that allows a convenient matrix solution. Once the surface acoustic pressure distribution is obtained from the Surface Helmholtz integral, then all the necessary information is available for the straightforward computation of any acoustic property or response of the body being studied. Radiated acoustic pressure can be calculated from equation (5) by letting point P be at any arbitrary location outside the body. Other difficulties associated with the numerical techniques necessary to model and solve given problems are discussed in the next section.

Examples

In this section, some of the difficulties associated with the Helmholtz integral are discussed and illustrated. These difficulties include surface modeling, techniques of overdetermining a problem, maximum element length criteria, and computation time. The examples include, in addition to the commonly used examples of the acoustic radiation from a uniformly dilating sphere and a transversely oscillating sphere, radiation from a piston set into the surface of a sphere. The results for all of the examples presented in this paper are given in nondimensional form in order to obtain general results.

Since the examples presented in this paper involve velocity distributions applied to spheres, the first step in the solution of these problems was the construction of a model that would accurately represent a spherical surface. Since the velocity and pressure distributions are to be applied to the modeled surfaces, if the model cannot accurately describe the geometry, it certainly cannot accurately describe a function over that geometry. Therefore, the accuracy of the computed surface area was used as a criterion to select the model. The surface areas were calculated with the same numerical integration schemes used later to evaluate the integrals of equation (5). Six different spherical models were constructed and the results of the surface area calculations are listed in Table 1. Even though the first four spherical models described in Table 1 are composed of quadratic elements, the calculations of the modeled surface areas show serious errors. The results shown for the last two models are much improved, suggested that quadratic quadralateral elements are better able to describe a spherical surface than are quadratic triangular elements. The model containing 24 quadratic quadralateral elements, illustrated in Fig. 1, was chosen for use in all the examples of this paper, unless otherwise noted.

Radiation From a Uniformly Dilating Sphere. Radiation from a uniformly dilating sphere is a basic problem of acoustics and has been studied extensively; see references [19-21]. The surface velocity distribution and the corresponding sound pressure radiation from a uniformly dilating sphere are given by

$$v_\nu(a,\theta,\phi) = U_0 \tag{6}$$

$$p(r/a)/z_0 U_0 = (a/r)[ika/(1+ika)]e^{-ika[(r/a)-1]}, \quad (r/a) \geq 1 \tag{7}$$

The exact solution (7) and the corresponding numerical results obtained from equation (5) for the surface pressure versus the frequency are shown in nondimensional form in Fig. 2. This figure clearly shows the failure of the surface Helmholtz integral in the neighborhood of the eigenfrequencies of the

Table 2 Results of the accuracy and symmetry study for the case of the oscillating sphere

Case	Location of Overdetermining Points x, y, z	Percent Difference from Theory ka=4.5 ϕ=0°	ka=4.5 ϕ=180°	ka=7.5 ϕ=0°	ka=7.5 ϕ=180°
1	none	-1199.3	-1199.3	127.7	127.7
2	0.0, 0.0, 0.0	-1199.3	-1199.3	127.7	127.7
3	0.0, 0.0, 0.2a	-2.9	-3.2	8.0	7.7
4	0.0, 0.0, 0.5a	-2.5	-2.5	78.1	74.8
5	0.0, 0.0, 0.8a	-5.0	-5.1	28.5	44.4
6	[0.0, 0.0, 0.2a; 0.0, 0.0,-0.2a]	-2.3	-2.3	-3.2	-3.2
7	[0.0, 0.0, 0.5a; 0.0, 0.0,-0.5a]	-2.3	-2.3	65.4	65.4
8	[0.0, 0.0, 0.8a; 0.0, 0.0,-0.8a]	-4.3	-4.3	15.9	15.9

related interior problem. For the case of a uniformly dilating sphere, these frequencies are the roots of the following Bessel function [12]

$$J_0(ka) = 0 \qquad (8)$$

or

$$ka \approx n\pi, \quad n = 1,2,3, \ldots$$

Figure 2 also shows the surface pressures obtained by overdetermining the Surface Helmholtz integral with the Interior Helmholtz integral, evaluated at a single point at the center of the sphere. A dramatic increase in accuracy can be seen, not only at the degenerate frequencies, but across the entire spectrum. Other researchers have suggested that in order to obtain a valid solution at one of these degenerate frequencies, one need only to interpolate solutions obtained at frequencies above and below the desired frequency. However, Fig. 2 demonstrates that the overdetermination of the Surface Helmholtz integral is necessary to achieve accurate results in a broad neighborhood of the interior eigenfrequencies.

Radiation From a Transversely Oscillating Sphere. Another basic problem in the study of acoustic radiation is that of a transversely oscillating sphere. The normal surface velocity distribution used to define this motion is given as

$$v_\nu(a,\theta,\phi) = U_0 \cos\phi \qquad (9)$$

and the corresponding theoretical solution for this problem is given as [19]

$$p(r/a,\phi)/z_0 U_0 = (a/r)^2 \cos\phi \, \frac{ka(i-kr)}{2(1+ika)-(ka)^2} \, e^{-ika[(r/a)-1]}, \quad (r/a) \geq 1 \qquad (10)$$

Figure 3 shows the surface pressure, at $\phi = 0$, versus the nondimensional frequency, ka. As in the case of the uniformly dilating sphere, the results near the interior eigenfrequencies clearly demonstrate the failure of the Surface Helmholtz formulation. In this case, the interior eigenfrequencies are given [12] as the roots of

$$J_1(ka) = 0 \qquad (11)$$

or

$$ka = 4.493409, \quad 7.725233, \ \ldots$$

The choice of an interior overdetermining point for this case is more difficult than that for the uniformly dilating sphere. As pointed out in reference [12], the overdetermining interior points cannot lie on the eigensurfaces of the related interior problem. A numerical experiment was performed to study the changes in accuracy and symmetry of the pressure response with the use of one and two overdetermining points in the interior of the oscillating sphere.

The results of eight distributions of internal overdetermining points, referred to as Cases 1–8, are presented in Table 2. All of the overdetermining points, if any, were located along the z-axis. These results illustrate the significance of the choice of the positions of interior points when overdetermining the Surface Helmholtz integral. A comparison of the results of Case 1 with any of the Cases 3–8 shows that a substantial in-

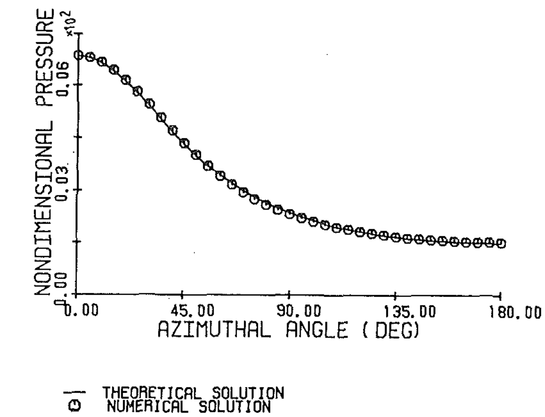

Fig. 5 Radiated nondimensional acoustic pressure versus ϕ for the case of the piston set in a sphere; $ka = 0.02$; $r/a = 2$

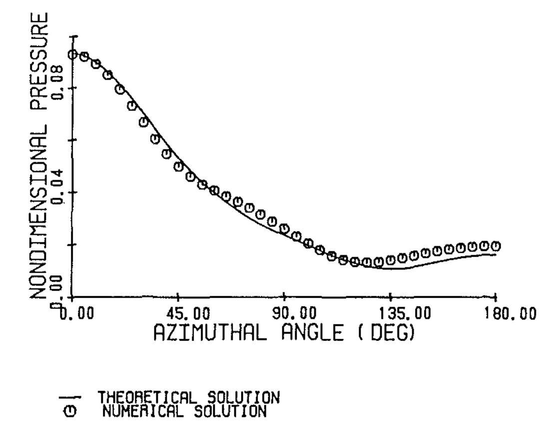

Fig. 6 Radiated nondimensional acoustic pressure versus ϕ for the case of the piston set in a sphere; $ka = 2.0$; $r/a = 2$

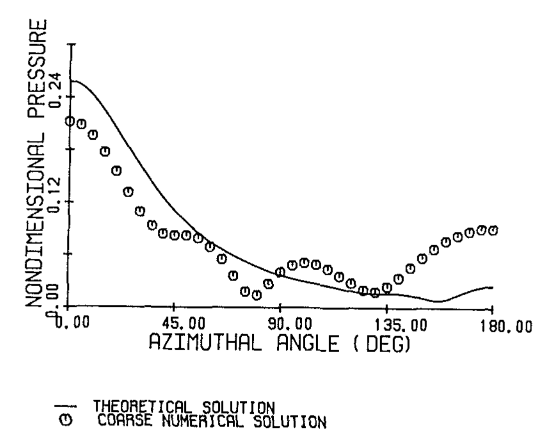

Fig. 7 Radiated nondimensional acoustic pressure versus ϕ for the case of the piston set in a sphere; coarse model; $ka = 5.0$; $r/a = 2$

Table 3 Computation time and storage requirements for various numerical models

Model			CPU Data	
Description	Number of Nodes	Number of Overdetermining Points	Time (sec)	Storage (pg-min)
50 linear quadralaterals	52	0	5.816	38.034
24 quadratic quadralaterals	74	0	6.567	42.984
24 quadratic quadralaterals	74	1	12.177	80.193
24 quadratic quadralaterals	74	2	12.270	80.834
24 quadratic quadralaterals	74	3	12.417	80.841
40 quadratic quadralaterals	122	0	19.623	129.569
40 quadratic quadralaterals	122	1	44.319	293.405
48 quadratic quadralaterals	146	0	29.547	195.870

crease in accuracy in the neighborhood of the degenerate frequencies occurs when the positions of the overdetermining points are selected properly. Examination of Table 2 shows that an interior location that increases the accuracy near one interior eigenfrequency may not be as effective at another eigenfrequency since the eigensurfaces are different for each interior mode. Indeed, Case 2 shows no increase in accuracy, implying that the location of the interior point in Case 2 is on the eigensurfaces of both test frequencies. The results given in Table 2 also show that a model which possesses symmetry about some plane must have its overdetermining points distributed symmetrically about that plane in order for the response of the model to maintain symmetry.

Radiation From a Piston in a Sphere. The last example considered is that of a piston, or a spherical cap, set into the surface of a rigid sphere as shown in Fig. 4. This problem is defined with the following normal velocity distribution

$$v_\nu(a,\theta,\phi) = \begin{cases} U_0, & 0 \le \phi \le \phi_0 \\ 0, & \phi_0 \le \phi \le \pi \end{cases} \tag{12}$$

The geometric model described earlier was modified to correctly model a circular area subtending 40 deg, $\phi_0 = 20°$, in this example. The theoretical solution, given in reference [21], is

$$p(r,\phi)/z_0 U_0 = \sum_{m=0}^{\infty} \frac{U_m P_m(\cos\phi)}{B_m(ka) + iC_m(ka)} [j_m(kr) + in_m(kr)] \tag{13}$$

where

$$U_m = [P_{m-1}(\cos\phi_0) - P_{m+1}(\cos\phi_0)]/2$$
$$B_m = n_{m-1}(ka) - (m+1)n_m(ka)/ka$$
$$C_m = (m+1)j_m(ka)/ka - j_{m-1}(ka)$$

j_m and n_m are the spherical Bessel and Neumann functions of order m, respectively, and P_m is the Legendre function of order m. For this example, comparison between the theoretical and the numerical calculations will be done using the radiated acoustic pressure patterns.

Figures 5-7 compare the radiation patterns obtained numerically using the modeled surfaces and the theoretical solutions. These radiation results are given for frequencies $ka = 0.02$, $ka = 2.0$, and $ka = 5.0$, at a radial distance of

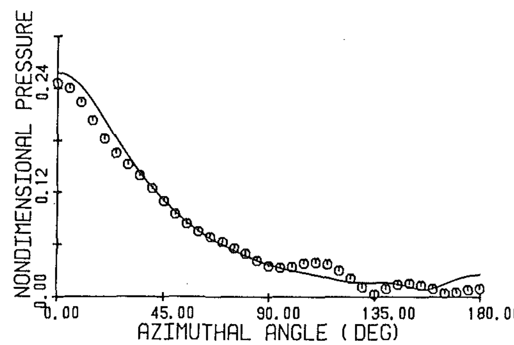

Fig. 8 Radiated nondimensional acoustic pressure versus ϕ for the case of the piston set in a sphere; fine model; $ka = 5.0$; $r/a = 2$

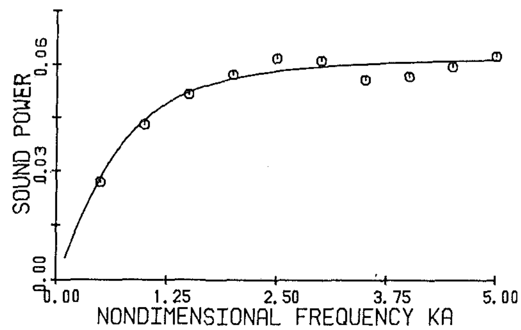

Fig. 9 Total radiated nondimensional sound power versus ka for the case of the dilating sphere

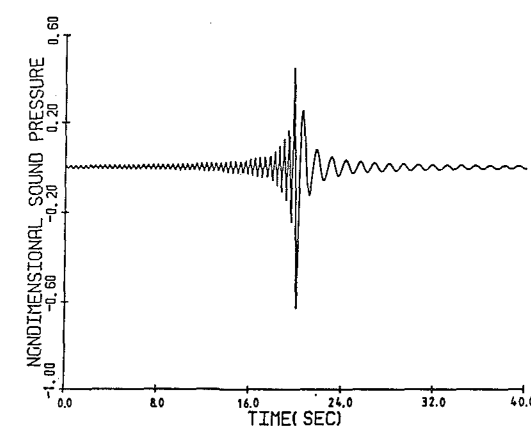

Fig. 10 Temporal acoustic response—Doppler effect $ka = 1.0$, $c = 1.0$, $v = 0.5$, stationary dilating sphere

$r/a = 2.0$ versus azimuthal angle. Agreement between theoretical and numerical results is excellent at the very low frequencies, and deteriorates as the frequency is increased. The reason for this is that the model is too coarse to allow accurate representation of the spatial surface pressure distribution at these frequencies. To verify this hypothesis, an improved spherical model was constructed with two extra rows of elements in the azimuthal direction. The radiation results from this model are compared to the theoretical calculations in Fig. 8. It is seen that these results are greatly improved over the results obtained with the more coarse model.

Discussion. The results presented in this section demonstrate the validity and the accuracy of the numerical implementation of the Helmholtz integral. Once the geometry and the surface velocity distribution are properly described, and the model is sufficiently overdetermined, the examples presented show excellent agreement with the results obtained analytically. The results presented for the piston set in a sphere are particularly interesting in that they support the notion that the use of higher-order elements can lead to improvements in accuracy with less computational effort. Chen and Schweikert [3] reported results similar to those shown in Fig. 6, but had to employ 320 constant triangular elements (320 nodes) to achieve the same degree of accuracy obtained here from a model having only 24 quadratic quadralateral isoparametric elements (74 nodes). Since the time necessary to solve matrix equations increases with the cubic power of the order of the matrix, it can be seen that an isoparametric formulation using higher-order elements results in significant reductions in computational time to achieve comparable accuracy.

The results obtained for the piston in a sphere also lead to a rule of thumb concerning the maximum allowable length of quadratic elements when modeling surfaces. These elements are defined by quadratic shape functions and cannot be expected to accurately approximate more than one half of a wavelength. In the cases considered, where $ka = 0.02$ and 2.0, the dimensions of the elements never exceeded 0.25λ and good results were obtained. However, when $ka = 5.0$, the elements spanned over 0.62λ with poor results. Since the surface velocity distribution was symmetric about the z-axis, the resulting surface pressure was also expected to be constant in any z = constant plane, verified by the lack of dependence on θ in the theoretical solution (13). The addition of two rows of elements in the azimuthal direction decreased the length of the elements in that direction to 0.42λ, thus improving the accuracy of the surface pressure results. This same criterion is expected to hold, although not as accurately, with linear quadralateral elements and when the element sizes do not exceed 0.25λ.

In this section, we have also seen dramatic increases in the accuracy of the results with the addition of overdetermining interior points. However, the use of overdetermining points introduces two difficult problems. The first of these problems resulting from the use of overdetermining interior points is the choice of location of the points. In reference [8], Schenck shows that in order to yield a unique solution near a degenerate frequency, the overdetermining points cannot all lie on the eigensurfaces of a related problem of the interior of the body. Therefore, when overdetermining the complex examples presented in reference [8], Schenck includes numerous interior points, distributed throughout the interior to insure that at least a few do not lie on the eigensurfaces. There is a particular need for an efficient and accurate method to determine the optimum location of interior points to overdetermine the Surface Helmholtz integral.

The other problem associated with the use of the overdetermined Helmholtz integral is that of increased computation time. In Table 3 is a list of the computation time and computer storage required on an Amdahl V8 main-frame computer for various numerical models. It can be seen from this data that the addition of a single overdetermining point doubles both the computer time and storage required to solve the system of equations resulting from the Helmholtz integral. The inclusion of additional interior points further increases computer time and storage, but by a relatively small amount. Optimization of the method used to solve the overdetermined system, or implementation of another method of solution, could result in a decrease of the computer time and storage required to solve a given problem.

Applications of Sound Power and Temporal Acoustic Response

The utility of the Helmholtz integral method is not limited to the determination of radiated sound pressure patterns. Once the acoustic pressure distribution is found on the surface of a body using equation (5), other characteristics of the acoustic field can be obtained fairly easily. The total radiated sound power and the temporal acoustic pressure response of dilating sphere are computed as examples.

Total Radiated Sound Power. In this section, the techniques that were developed earlier in this paper are used to present a convenient method of obtaining the total sound power radiated from an arbitrarily vibrating object.

The total sound power radiated from a vibrating object is defined as

$$P = 1/2 \int_S \mathrm{Re}[p^* v_\nu] d\sigma \tag{14}$$

where (*) denotes a complex conjugate. Examination of equation (14) shows that the radiated sound power depends on the surface acoustic pressure distribution, the surface normal velocity profile, and the surface geometry. Following the methods discussed earlier, equation (14) can be written in terms of interpolation functions as

$$P = 1/2 \sum_{m=1}^{M} \sum_{n=1}^{N} \mathrm{Re}[p_n{}^* v_{\nu n}] \int_{S_m} h_n J_n d\sigma. \tag{15}$$

Equation (15) can then be evaluated following the determination of the complex surface acoustic pressure distribution by the Surface Helmholtz integral, equation (5). Sound power calculation given by equation (15) is applied to the case of a dilating sphere, and the results are compared to the theoretical values in Fig. 9. The accuracy of these calculations is comparable to the accuracy of the surface pressure distribution for the given problem.

Temporal Acoustic Response. The need to solve problems of acoustic radiation in the time domain often arises in industrial and research work. The general Helmholtz integral in equation (2) is given in the frequency domain for steady-state acoustic radiation from the surface of an arbitrary body. The corresponding general time-dependent acoustic response from arbitrary bodies can be obtained by one of the following two methods.

The first of these involves the use of the temporal form of the Helmholtz integral. This integral is obtained from the Helmholtz integral through an inverse Fourier transform and is given as

$$\begin{aligned}\{4\pi + \textstyle\int_S [\partial(1/r)/\partial\nu] d\sigma\} p(P,t) &= \textstyle\int_S (\rho_0/r)\{d[v_\nu(t-r/c)]/dt\} d\sigma \\ &\quad - \textstyle\int_S \cos(r,\nu)[(1/cr)(d/dt) + (1/r^2)] p(t-r/c) d\sigma. \end{aligned} \tag{16}$$

In order to solve a general acoustic radiation problem, one needs to know not only the time-dependent acoustic pressure function, but also its time derivative. Since this integral is but one equation involving two unknown functions, it can be solved only for the special cases where the time derivative of the surface pressure can be expressed as a simple function of the surface pressure itself.

The second method of obtaining sound pressure in the time domain can be done by either (*i*) inverting the sound pressure at the field point obtained in the frequency domain from the Helmholtz integral or (*ii*) by inverting the surface pressures obtained by the Helmholtz integral and then using the temporal Helmholtz integral in equation (16) to calculate the acoustic radiation at the field points. If the radiation at many field points is required, the latter approach is recommended since it will reduce the computer storage requirements from multiple values of pressure at each frequency to one for each point in time.

The main problems involved in the computation of time-dependent acoustic response are the length and complexity of the calculations and the massive amount of data that must be handled. In general, the velocity distribution and the calculated acoustic pressure have an infinite number of frequency components. As the frequency is increased, the number of elements representing the structure must increase in accordance with the guidelines on element size developed earlier. These problems can be alleviated in special cases, such as steady-state harmonic vibration, but are formidable obstacles to general results.

As an example of temporal acoustic radiation, an acoustic Doppler effect is illustrated. A stationary harmonically dilating sphere is approached and is passed by a moving receiver. This example can be solved conveniently by any of the methods discussed in this section since the surface velocity has but one frequency component. The latter method just described was used since the time derivatives of the pressure differs from the pressure itself by a factor of $i\omega$. The sphere radiates at a nondimensional frequency of $ka = 1.0$ ($f = 1.59$ cps) and the acoustic pressure calculated corresponds to that observed at a receiver moving past the sphere at a speed of one-half the speed of sound. The frequency shift is governed by (see, for example, reference [21])

$$f' = f(1 - v/c) \tag{17}$$

where c is the speed of sound, f is the source frequency, v is the velocity of the receiver and f' is the apparent frequency observed by the receiver. Figure 10 shows the results of the numerical calculations. As the receiver approaches the source, the calculated apparent frequency is 2.38 cps and as the receiver moves away from the source, the received frequency shifts to 0.79 cps, both precisely as predicted by equation (17).

Conclusions

In this paper, the overdetermined, isoparametric formulation of the Helmholtz integral was shown to be accurate, versatile, and easy to implement. Guidelines have been developed and tested concerning the modeling of surfaces and for the efficient solution of problems by this method. Additional areas of study include an efficient method to determine the location and number of the overdetermining interior points and the optimization of the methods used for the solution of overdetermined sets of simultaneous linear equations.

Acknowledgment

The authors would like to acknowledge the support of the National Science Foundation for this research under a grant from the Dynamic Systems and Control Program.

References

1 Oestreicher, H., 1957, "Representation of the Field of an Acoustic Source as a Series of Multipole Fields," *J. Acoust. Soc. Am.*, Vol. 29, pp. 1219–1222.

2 Horton, C. W., and Innis, G. S., 1961, "The Computation of Far-Field Radiation Patterns From Measurements Made Near the Source," *J. Acoust. Soc. Am.*, Vol. 33, pp. 877–880.

3 Chen, L. H., and Schweikert, D. G., 1963, "Sound Radiation From an Arbitrary Body," *J. Acoust. Soc. Am.*, Vol. 35, pp. 1626–1632.

4 Chertock, G., 1964, "Sound Radiation From Vibrating Surfaces," *J. Acoust. Soc. Am.*, Vol. 36, pp. 1305–1313.

5 Copley, L. G., "Integral Equation Method for Radiation From Vibrating Bodies," *J. Acoust. Soc. Am.*, Vol. 41, pp. 807–816.

6 Copley, L. G., 1968, "Fundamental Results Concerning Integral Representations in Acoustic Radiation," *J. Acoust. Soc. Am.*, Vol. 44, pp. 28–32.

7 Ursell, F., 1973, "On the Exterior Problems of Acoustics," *Proc. Cambridge Phil. Soc.*, Vol. 74, pp. 117–125.

8 Schenck, H. A., 1968, "Improved Integral Formulation for Acoustic Radiation Problems," *J. Acoust. Soc. Am.*, Vol. 44, pp. 41–58.

9 Ursell, F., 1978, "On the Exterior Problems of Acoustics: II," *Math. Proc. Camb. Phil. Soc.*, Vol. 84, pp. 545–548.

10 Brod, K., 1984, "On the Uniqueness of Solution for All Wavenumbers in Acoustic Radiation," *J. Acoust. Soc. Am.*, Vol. 76, pp. 1238–1243.

11 Bell, W. A., Meyer, W. L., and Zinn, B. T., 1977, "Predicting the Acoustics of Arbitrarily Shaped Bodies Using an Integral Approach," *AIAA Journal*, Vol. 15, pp. 813–820.

12 Koopman, G. H., and Benner, H., 1982, "Method for Computing the Sound Power of Machines Based on the Helmholtz Integral," *J. Acoust. Soc. Am.*, Vol. 71, pp. 78–89.

13 Benner, H., and Koopman, G. H., 1981, "Sound Power Prediction Using the Helmholtz-Kirchhoff Integral Equation," ASME Paper 81-WA/NCA-4.

14 Seybert, A. F., Soenarko, B., Rizzo, F. J., and Shippy, D. J., 1982, "Application of the BIE Method to Sound Radiation Problems Using an Integral Approach," ASME Paper 82-WA/NCA-1.

15 Seybert, A. F., Soenarko, B., Rizzo, F. J., and Shippy, D. J., 1985, "An Advanced Computational Method for Radiation and Scattering of Acoustic Waves in Three Dimensions," *J. Acoust. Soc. Am.*, Vol. 77, pp. 362–368.

16 Sokolnikoff, I. S., and Redheffer, R. M., 1966, *Mathematics of Physics and Modern Engineering*, McGraw-Hill, New York, pp. 500–507.

17 Bathe, K., 1982, *Finite Element Procedures in Engineering Analysis*, Prentice-Hall, New Jersey.

18 Cowper, G. R., 1973, "Gaussian Quadrature Formulas for Triangles," *Int. J. Num. Meth. in Eng.*, Vol. 7, pp. 405–408.

19 Pierce, A. D., 1981, *Acoustics*, McGraw-Hill, New York.

20 Skudruzk, E., 1971, *The Foundations of Acoustics*, Springer-Verlag/Wien.

21 Morse, P. M., and Ingard, K. U., 1968, *Theoretical Acoustics*, McGraw-Hill, New York.